Persistent Ferromagnetism and Topological Phase Transition at the Interface of a Superconductor and a Topological Insulator

Wei Qin and Zhenyu Zhang[*]

International Center for Quantum Design of Functional Materials (ICQD), Hefei National Laboratory for Physical Sciences at the Microscale (HFNL), and Synergetic Innovation Center of Quantum Information and Quantum Physics, University of Science and Technology of China, Hefei, Anhui 230026, China

At the interface of an s-wave superconductor and a three-dimensional topological insulator, Majorana zero modes and Majorana helical states have been proposed to exist respectively around magnetic vortices and geometrical edges. Here we first show that randomly distributed magnetic impurities at such an interface will induce bound states that broaden into impurity bands inside (but near the edges of) the superconducting gap, which remains open unless the impurity concentration is too high. Next we find that an increase in the superconducting gap suppresses both the oscillation magnitude and the period of the Ruderman-Kittel-Kasuya-Yosida interaction between two magnetic impurities. Within a mean-field approximation, the ferromagnetic Curie temperature is found to be essentially independent of the superconducting gap, an intriguing phenomenon due to a compensation effect between the short-range ferromagnetic and long-range antiferromagnetic interactions. The existence of robust superconductivity and persistent ferromagnetism at the interface allows realization of a novel topological phase transition from a nonchiral to a chiral superconducting state at sufficiently low temperatures, providing a new platform for topological quantum computation.

Introduction.—Non-Abelian fermions have attracted much attention because of their potential applications in topological quantum computation (TQC) [1,2]. One common physical entity obeying non-Abelian braiding statistics is the zero-energy Majorana fermion [3], which is its own antiparticle described by $\gamma = \gamma^{\dagger}$. In condensed matter physics, a chiral topological superconductor (TSC) [4] is characterized by the existence of two types of Majorana fermions, chiral Majorana edge modes and a single Majorana zero mode surrounding a magnetic vortex; the latter can be manipulated for realization of TQC [5–8]. The simplest chiral TSC is a spinless $p_x + ip_y$ superconductor (SC) or superfluid [9]; however, it is difficult to quench the spin degrees of freedom in order to realize spinless SCs.

Recently, it was proposed that the proximity-induced superconductivity on the surface of a topological insulator (TI) deposited on a conventional s-wave SC possesses a $p_x + ip_y$ pairing feature [10]. The nonchiral nature of such a spinful SC is characterized by the existence of Majorana helical edge states and a pair of Majorana zero modes surrounding a magnetic vortex. To convert such a TSC into a chiral one, time reversal symmetry (TRS) must be broken. Two schemes have been proposed to break TRS, both relying on the effect of a Zeeman field. The first consists of a SC-TI-magnet junction [10]; in the second scheme, the TI can be further replaced by a traditional semiconducting thin film with strong Rashba spin-orbit coupling (SOC) [11,12]. These intriguing proposals have motivated extensive experimental efforts for the detection of Majorana

fermions [13–15], but so far definitive proof of their existence remains controversial. Here we note that both schemes face the inherent challenge that the proximity-induced Zeeman field decays rapidly through the TI or semiconductor thin film.

In this Letter, we introduce an alternative and conceptually new scheme to realize a chiral TSC within a simpler structure, achieved by randomly doping magnetic impurities directly at a TI-SC interface (see Fig. 1). We first show that these magnetic impurities will induce bound states that broaden into impurity bands inside (but near the edges of) the superconducting gap, which remains open unless the impurity concentration is too high. Next we find that an increase in the superconducting gap suppresses both the oscillation magnitude and the period of the Ruderman-Kittel-Kasuya-Yosida (RKKY) interaction between two magnetic impurities mediated by BCS quasiparticles.
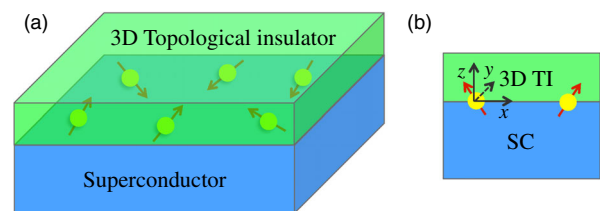
FIG. 1 (color online). (a) Schematic of randomly distributed magnetic impurities at the interface of a 3D TI and a superconductor. (b) Side view of the TI-SC heterostructure exhibiting the positions of the magnetic impurities.

The ferromagnetic Curie temperature is found to be essentially independent of the superconducting gap due to a compensation effect between the short-range ferromagnetic and the long-range antiferromagnetic interactions. The existence of persistent ferromagnetism at the interface provides a strong and uniform Zeeman field for the realization of a chiral TSC. In particular, by investigating the edge states and the corresponding first Chern number [16], we reveal a topological phase transition from a nonchiral to a chiral TSC at sufficiently low temperatures. These findings, in principle, provide a new and more appealing platform for TQC.

Theoretical model.—The surface states of strong TIs are described by the time reversal invariant Hamiltonian $H_0 = \sum_k \psi_k^\dagger (\nu_F \vec{\sigma} \cdot \vec{k} - \mu)\psi_k$. Here $\psi_k^\dagger = (c_{k\uparrow}^\dagger, c_{k\downarrow}^\dagger)$, $\vec{\sigma} = (\sigma_x, \sigma_y)$ are the Pauli spin matrices, μ is the chemical potential, and ν_F is Fermi velocity, given by 4.08 eV Å for Bi_2Se_3 [17] and 3.70 eV Å for Sb_2Te_3 [18]. By depositing a TI on the surface of an *s*-wave SC, the proximity-induced pairing Hamiltonian is given as $H_p = \sum_k (\Delta c_{k\uparrow}^\dagger c_{-k\downarrow}^\dagger +$ H.c.). Here $\Delta = \Delta_0 e^{i\phi}$ is the superconducting gap with phase ϕ. The states at the TI-SC interface can then be described by [10]

$$H_0 = \frac{1}{2}\sum_k \Psi_k^\dagger \mathcal{H}(\vec{k})\Psi_k,$$

$$\mathcal{H}(\vec{k}) = (\nu_F \vec{\sigma} \cdot \vec{k} - \mu)\tau_z - \Delta_0(\tau_x \cos\phi - \tau_y \sin\phi), \quad (1)$$

where $\Psi_k^\dagger = (c_{k\uparrow}^\dagger, c_{k\downarrow}^\dagger, c_{-k\downarrow}, -c_{-k\uparrow})$ are four-dimensional field operators in the Nambu spinor basis. TRS and particle-hole symmetry are expressed as $\Theta = i\sigma_y K$ and $\Xi = \sigma_y \tau_y K$, which satisfy $[\Theta, \mathcal{H}] = 0$ and $\{\Xi, \mathcal{H}\} = 0$ at Γ point of the Brillouin zone, respectively, where K is the complex conjugate operator.

At the microscopic level, we treat the *s-d* interaction between a magnetic impurity located at $\vec{R}_i$ and the electrons at the TI-SC interface to be isotropic, described by $H_{sd}^i = -J(\vec{\sigma} \cdot \vec{S})\delta(\vec{r} - \vec{R}_i)$, where $\vec{\sigma} = (\sigma_x, \sigma_y, \sigma_z)$ is the real electron spin and $\vec{S}$ is the spin of the magnetic impurity. In Nambu notations, the interaction Hamiltonian can be rewritten as

$$H_{sd} = -\frac{J}{2}\sum_{kk'} \Psi_k^\dagger (\vec{S} \cdot \vec{\sigma})\tau_0 \Psi_{k'}, \quad (2)$$

where J denotes the *s-d* exchange coupling strength at the interface, estimated to be 0.1–0.5 eV [18–20]. Hamiltonian (2) describes the interaction between the magnetic impurities and BCS quasiparticles, which, together with Hamiltonian (1), define our theoretical model and the starting point of this study.

Magnetic impurity-induced states.—In *s*-wave SCs, a magnetic impurity will induce quasiparticle bound states inside the superconducting gap [21,22]. These intragap states will grow into impurity bands at finite concentrations

of the magnetic impurities and will finally suppress the superconductivity completely [22]. In this section, we first study a single magnetic impurity-induced state at the TI-SC interface using the *T*-matrix technique [23]. The matrix form of the retarded Green's function of Eq. (1) reads

$$\hat{G}_0^{-1}(\omega, \vec{k}) = \omega + i\delta - \mathcal{H}(\vec{k}). \quad (3)$$

The *T* matrix is found using the Lippmann-Schwinger equation

$$\hat{T}(\omega) = \hat{U} + \hat{U}\hat{G}_0(\omega, 0)\hat{T}(\omega), \quad (4)$$

where $\hat{G}_0(\omega, 0)$ is the Green's function in real space and $\hat{U} = -(J/2)(\vec{S} \cdot \vec{\sigma})\tau_0$ in our system. The algebra is simplest for $\mu = 0$ and $\phi = 0$, where the Green's function in real space is given by the Fourier transformation of Eq. (3). For $\vec{r} \to 0$, the Green's function takes the following asymptotic form:

$$\hat{G}_0(\omega, 0) = f(\omega, \Delta_0)(\omega - \Delta_0\tau_x), \quad (5)$$

where $f(\omega, \Delta_0) = [\ln(\sqrt{\Delta_0^2 - \omega^2}/2W) + \chi]v/(2\pi\nu_F^2)$, v is the volume of the lattice primitive cell, W is the band cutoff, and χ is the Euler-Mascheroni constant. From the algebraic relations of Eqs. (4) and (5), we find two poles of the *T* matrix within $|\omega| < \Delta_0$ which are determined by the self-consistent equation $\omega = \pm[\Delta_0 + 2/JSf(\omega, \Delta_0)]$, giving rise to two impurity bound states inside the superconducting gap. By solving the equation, we find that these bound states are located very close to the superconducting gap edges. This is because the *s-d* coupling strength J at the interface is rather weak compared to the case of bulk materials. In addition, the low density of states (DOS) associated with the TI surface state will further weaken the consequence of the coupling between the magnetic impurity and the TI surface electrons.

Next we will consider the case at finite impurity concentrations. The Green's function averaged over randomly distributed magnetic impurities is found from the Dyson's equation

$$\hat{G}^{-1}(\omega, \vec{k}) = \hat{G}_0^{-1}(\omega, \vec{k}) - \hat{\Sigma}(\omega, \vec{k}), \quad (6)$$

where $\hat{\Sigma}$ is the self-energy given approximately as $\hat{\Sigma}(\omega, \vec{k}) = xT(\omega)$, x is the concentration of the magnetic impurities, and $T(\omega)$ is determined by Eq. (4) with the substitution of $\hat{G}_0(\omega, 0)$ by the full Green's function $\hat{G}(\omega, 0)$. The DOS of the TI-SC interface doped with a finite concentration of magnetic impurities is given as $\rho(\omega) = -(1/2\pi)\text{Im}\{\text{Tr}[\hat{G}(\omega)\tau_0]\}$, where the full Green's function $\hat{G}(\omega)$ can be obtained self-consistently from Eq. (6) (see details in the Supplemental Material [24]).

As illustrated in Fig. 2(a), an increase in the concentration of randomly distributed magnetic impurities suppresses the superconductivity of the TI-SC interface. However, the superconducting gap is still robust even
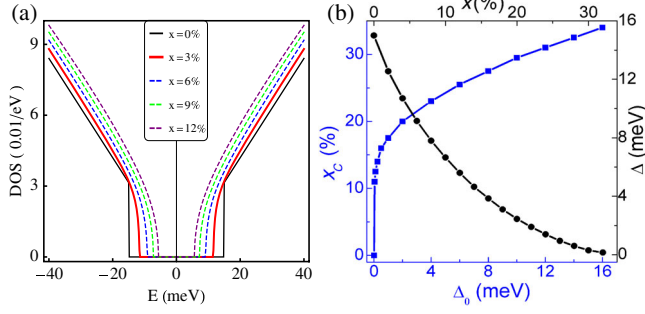
FIG. 2 (color online). (a) DOS as a function of the electron energy E at different x. (b) Renormalized superconducting gap as a function of x (black), and the critical concentration x_c for systems with different superconducting gaps (blue).

when the concentration is more than ten percent. The superconducting gap as a function of the magnetic doping concentration is also plotted in Fig. 2(b). In order to study the robustness of the superconductivity at the TI-SC interface, we define x_c as the critical concentration above which the superconducting gap closes. As shown in Fig. 2(b), x_c is above ten percent for nearly all of the gap range studied. Such a large critical concentration is due directly to the weak couplings between the magnetic impurities and the TI-SC interface electrons.

RKKY interaction and ferromagnetism.—In this section, we focus on the magnetic properties of the TI-SC interface doped with randomly distributed magnetic impurities. In order to study the collective magnetic behaviors of such systems, we first consider the RKKY interaction between two magnetic impurities mediated by the BCS quasiparticles. Hamiltonian (1) can be mapped into a two-band spinless $p_x + ip_y$ Hamiltonian as

$$H_0 = \sum_{km}\xi_{km}\alpha_{km}^\dagger\alpha_{km} - \frac{1}{2}(m\Delta e^{i\theta_k}\alpha_{km}^\dagger\alpha_{-km}^\dagger + \text{H.c.}), \quad (7)$$

where $\xi_{km} = m v_F k - \mu$ are the Dirac electron spectra, $m = \pm 1$ are the band indices, and $\alpha_{km} = (me^{i\theta_k}c_{k\uparrow} + c_{k\downarrow})/\sqrt{2}$. Using the same basis set, Hamiltonian (2) can be rewritten as

$$H_{sd}^i = -J\sum_{mm'kk'} e^{i(\vec{k}'-\vec{k})\cdot\vec{R}_i}(\vec{S}_i \cdot \vec{\sigma}_{km;k'm'})\alpha_{km}^\dagger\alpha_{k'm'}, \quad (8)$$

where $\vec{\sigma}_{km;k'm'}$ are the spin matrices.

In the following, we treat the many-body problem using perturbation theory. The corrected ground state energy due to s-d hybridization is $E = \langle\Omega|TH_0S(\infty,-\infty)|\Omega\rangle$, where T is the time-order operator and the S matrix is defined as $S(t,t') = T\exp\left[-i\int_{t'}^t dt_1\hat{H}_{sd}(t_1)\right]$. The BCS ground state is $|\Omega\rangle = \prod_{km}(u_{km} + \nu_{km}\alpha_{km}^\dagger\alpha_{-km}^\dagger)|0\rangle$, where u_{km} and ν_{km} are determined by the Bogoliubov transformation and $|0\rangle$ is the vacuum state. The normalization condition $\langle\Omega|\Omega\rangle = 1$ is ensured by $|u_{km}|^2 + |\nu_{km}|^2 = 1$. By expanding the S matrix to the second order in H_{sd} and considering only the

loop approximation between two different magnetic impurities i and j, the RKKY interaction can be effectively written as

$$H_{ij}^{\text{int}} = F_1(R,\mu)(S_i^z S_j^z + S_i^y S_j^y) + F_2(R,\mu)S_i^x S_j^x$$
$$+ F_3(R,\mu)(\vec{S}_i \times \vec{S}_j)_x, \quad (9)$$

where

$$F_\alpha(R,\mu) = -\frac{J^2 v^2}{32\pi^2}\int_0^{k_c} dk dk'\sum_{mm'}D_{km;k'm'}^\alpha(R)$$
$$\times \frac{kk'(E_{km}E_{k'm'} - \xi_{km}\xi_{k'm'} - \Delta^2)}{E_{km}E_{k'm'}(E_{km} + E_{k'm'})}, \quad (10)$$

with $\alpha = 1$, 2, or 3, k_c is a large momentum cutoff, and $E_{km} = \sqrt{\xi_{km}^2 + \Delta^2}$ is the excitation spectrum of the BCS quasiparticles, which can be obtained by diagonalizing Hamiltonian (7). In Eq. (10), we also have $D_{km;k'm'}^{1(2)}(R) = J_0(kR)J_0(k'R) - (+)mm'J_1(kR)J_1(k'R)$, $D_{km;k'm'}^3(R) = m'J_0(kR)J_1(k'R) + mJ_1(kR)J_0(k'R)$, and $J_{0,1}(x)$ are the Bessel functions of the first kind. On a face level, the anisotropic RKKY interaction is qualitatively similar to that on a TI surface [20] due to the SOC effects in both systems. However, the presence of the superconductivity introduces crucial differences, as reflected in Eq. (10) and discussed in more detail below.

In general, the oscillation period of the RKKY interaction is determined by the Fermi wavelength $\lambda_F = 1/k_F$. As shown in Fig. 3(a), an increase in the superconducting gap Δ suppresses both the oscillation magnitude and the period of the RKKY interaction, exhibiting a fast decay of the long-range part of the interaction to be close to zero. These behaviors stem from two physical aspects. First, the proximity-induced superconductivity will introduce a gap of 2Δ at the Fermi level by forming Cooper pairs; because every excitation of the quasiparticles has to overcome the superconducting gap, the corresponding RKKY interaction mediated by the quasiparticles will be suppressed in magnitude, especially the long-range part. Second, since
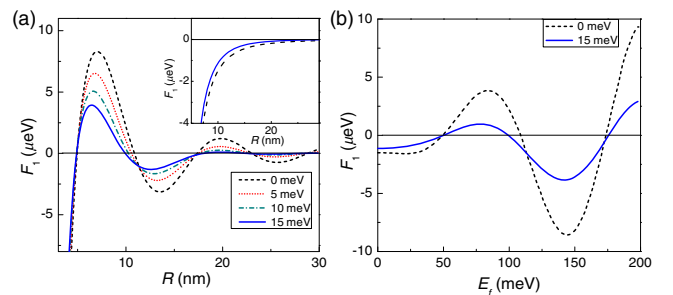
FIG. 3 (color online). RKKY interaction between two magnetic impurities as a function of the separation R and the Fermi energy E_f calculated with $J = 0.5$ eV, $E_f = 100$ meV for (a) and $R = 10$ nm for (b). The insert in (a) shows the case for the Fermi surface located at the Dirac point.

the occupied states close to the superconducting gap dominate the contribution to the RKKY interaction, the corresponding wave vector is smaller than k_F, leading to a modification in the oscillation period. In Fig. 3(b), the Fermi energy dependence of the RKKY interaction is also presented.

From the RKKY interaction described above, we can obtain the collective behavior of the magnetic impurities under the realistic assumption that their spatial distribution is random. The positional randomness combined with Eq. (9) leaves the in-plane interaction frustrated (for a more thorough discussion on the in-plane magnetization, see the second section of the Supplemental Material [24]), while the ferromagnetic interaction between the z components of the local spins can be optimized. Accordingly, a z-direction-aligned ferromagnetic ground state is expected for the multiple magnetic impurity system, even though the atomic s-d hybridization is isotropic. The mean-field (MF) virtual crystal approximation can be employed to estimate the Curie temperature T_c^{MF}, given as [26,27]

$$k_B T_c^{MF} = \frac{2x}{3} \sum_{i(i \neq 0)} J_{0i}, \qquad (11)$$

where the sum extends over the virtual sites and x is the concentration of the magnetic impurities on those virtual sites. The continuum limit is reached with $k_B T_c^{MF} = (4\pi n_i/3) \int_0^\infty r J(r) dr$, where n_i is the density of the magnetic impurities. For $Bi_2 Se_3$, the virtual sites are the locations of the Bi atoms. By setting $x = 3\%$, $a = 4.14$ Å, $J = 0.5$ eV, and $E_f = 0.1$ eV, the estimated T_c for different superconducting gaps is listed in Table I. As shown in Fig. 3(a), the behaviors of the RKKY interaction are dramatically influenced by the superconducting gap, while the MF T_c shows nearly constant values. These intriguing phenomena stem from a subtle compensation effect between ferromagnetism and antiferromagnetism: For $\Delta = 0$, the magnitude of the long-range RKKY interaction shows a spatial dependence as $1/R^2$ [20], favoring antiferromagnetism, while the short-range correlation always favors ferromagnetism. For $\Delta \neq 0$, both the magnitude and the long-range oscillation of the RKKY interaction will be suppressed, which again mutually compensate each other, leading to robust Curie temperatures, as listed in Table I.

Chiral TSC and topological phase transition.—Now we discuss the topological state of the TI-SC interface in the presence of random magnetic impurities. Based on the DOS study, we already found that the proximity-induced superconductivity is robust unless the impurity concentration is

too high. From the MF approximation, we can therefore estimate the effective exchange field induced by the randomly distributed magnetic impurities, given by $V_{ex} = 3Jx\langle S_z \rangle$. Within the picture that a given magnetic impurity interacts with an effective Zeeman field $B_{eff} = x\sum_i J_{0i}\langle S_z \rangle$ defined by all of the other magnetic impurities, its magnetic polarization is given by $\langle S_z \rangle = SB(B_{eff}S/k_BT)$, where $B(x) = (1 + 1/2S)\coth((1 + 1/2S)x) - (1/2S)\coth((1/2S)x)$ is the Brillouin function. Therefore, the self-consistent solution of $\langle S_z \rangle$ and B_{eff} can give rise to the temperature dependence of V_{ex}, as shown in Fig. 4(a). Importantly, the very existence of the robust superconductivity and V_{ex} characterize the chiral nature of the superconducting system, as further elaborated below.

In an analogy with Ref. [10], by defining the Bogoliubov quasiparticle operators as $\gamma(\mathbf{r}) = \sum_\sigma u_\sigma(\mathbf{r})\psi_\sigma^\dagger(\mathbf{r}) + \nu_\sigma(\mathbf{r})\psi_\sigma(\mathbf{r})$ and solving the BdG equation $\mathcal{H}_{BdG}\Psi(\mathbf{r}) = E\Psi(\mathbf{r})$ with $\Psi(\mathbf{r}) = [\nu_\uparrow(\mathbf{r}), \nu_\downarrow(\mathbf{r}), u_\downarrow(\mathbf{r}), u_\uparrow(\mathbf{r})]^T$ at geometrical edges, we can find two types of Majorana edge states by varying V_{ex}. First, for $\sqrt{\mu^2 + \Delta^2} > V_{ex} > \mu$, there are two helical edge states, given by $\Psi_\pm(x) = (1/\mathcal{N}_\pm)(\sqrt{V^-}, \mp i\sqrt{V^+}, \mp e^{i\phi}\sqrt{V^+}, ie^{i\phi}\sqrt{V^-})^T e^{-\eta x}$, where $V^\pm = V_{ex} \pm \mu$, $\eta = (\Delta \pm \sqrt{V^+V^-})/\nu_F$, and $\mathcal{N}_\pm$ are the normalization parameters. It is easy to verify that $\gamma^\dagger(k_y) = \gamma(-k_y)$, which implies that the solutions are Majorana edge modes. In order to give an intuitional picture of the helical edge states, we evaluate the low-energy "$k \cdot p$" Hamiltonian as $\mathcal{H}_h = \sqrt{1 - (\mu/V_z)^2}\nu_F k_y \tau_z$, where τ_z is the Pauli matrix. Second, for $V_{ex} > \sqrt{\mu^2 + \Delta^2}$, there are two degenerate chiral Majorana edge states $\Psi_\pm(x) = (1/\mathcal{N}_\pm)(\sqrt{V^-}, -i\sqrt{V^+}, \mp e^{i\phi}\sqrt{V^+}, \pm ie^{i\phi}\sqrt{V^-})^T e^{\mp\eta x}$, where $\mathcal{N}_\pm$ are the normalization parameters. The chiral nature can be illustrated by the low-energy $k \cdot p$ Hamiltonian, given by $\mathcal{H}_c = \sqrt{1 - (\mu/V_z)^2}\nu_F k_y$. Therefore, by varying the exchange field V_{ex}, we can expect a topological phase transition from a helical to a chiral TSC at $V_{ex} = \sqrt{\mu^2 + \Delta^2}$, and the corresponding transition temperature is marked by T_s in Fig. 4(a).

As a quantitative measure for the occurrence of the topological phase transition, we calculate the first Chern number for systems before and after the transition. The first Chern number can be defined as the integral of the Berry curvature over the first Brillouin zone [16]: $\mathcal{C}_1 = (1/2\pi)\int_{BZ}(\partial_{k_x}\mathcal{A}_{k_y} - \partial_{k_y}\mathcal{A}_{k_x})d\mathbf{k}$, where $\mathcal{A}_{k_\alpha} = -i\sum_n\langle u_n(\mathbf{k})|\partial_{k_\alpha}|u_n(\mathbf{k})\rangle$ is the Berry connection, $\alpha = x, y$, and the index n runs over all of the occupied states. Hamiltonian (1) can be regularized on a square lattice with the substitution $p_{x,y} \to a^{-1}\sin(p_{x,y}a)$, where a is the lattice constant. The results for $\mu = 0$ are shown in Fig. 4(b). There are two sets of subbands due to spin degrees of freedom. When $V_{ex} < \Delta$, the resulting Chern numbers from the two sets are equal in magnitude but opposite in sign and the total Chern number $\mathcal{C}_1 = 0$

TABLE I. Robust Curie temperatures for systems of different superconducting gaps, obtained with $x = 3\%$.

Δ	0 meV	5 meV	10 meV	15 meV
T_c^{MF}	3.282 K	3.228 K	3.234 K	3.243 K
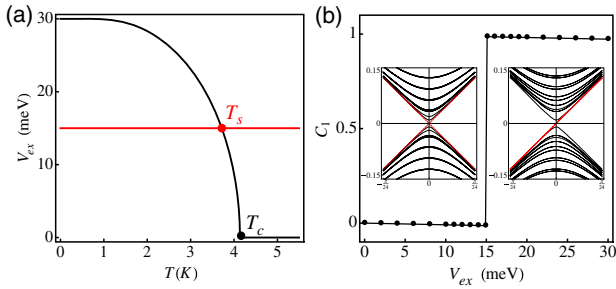
FIG. 4 (color online). (a) The effective exchange field V_{ex} (black line) and the superconducting gap Δ (red line) as a function of the temperature. T_s indicates the topological phase transition temperature, which is below the ferromagnetic Curie temperature T_c. (b) The Chern number as a function of V_{ex}. The insets illustrate the bulk band spectra (black solid lines) and edge states (red dashed lines) in the helical and chiral phases, calculated with $V_{\mathrm{ex}} = 5$ and 25 meV, respectively. Other parameters include $\Delta = 15$ meV, $J = 0.5$ eV, $E_f = 0$ meV, and $x = 3\%$.

signifies a nonchiral TSC state. When $V_{\mathrm{ex}} > \Delta$, one set of the subbands will be inverted by the exchange field and the corresponding Chern number will also reverse sign, resulting in $\mathcal{C}_1 = 1$, indicating a chiral TSC state.

So far, we have focused on realizing chiral TSC at the TI-SC interface. As an extension, here we also briefly discuss the proposed scheme in connection with recent experiments [28,29]. When Bi_2Se_3 was grown on the d-wave SC of $Bi_2Sr_2CaCu_2O_{8+\delta}$, an s-wave superconducting gap of ~15 meV was observed on the top surface of the TI [29]. Based on these experiments, we expect that the proposed mechanism can also be exploited to realize chiral TSCs on tops of TI-SC heterostructures.

In summary, we have proposed an alternative and conceptually simpler scheme to realize a chiral TSC, achieved by doping magnetic impurities directly at a TI-SC interface. We have found that, at physically realistic concentrations of randomly distributed magnetic impurities, the proximity-induced superconductivity is robust, and the RKKY interaction gives rise to a persistent ferromagnetic state independent of the superconducting gap. The ferromagnetic state can naturally provide a strong and uniform exchange field, which in turn breaks the TRS, driving the system from a nonchiral into a chiral TSC phase at sufficiently low temperatures. The proposed scheme is, in principle, also applicable on top of a TI-SC heterostructure, or when the TI is replaced by a normal semiconductor with strong Rashba SOC. These findings, therefore, provide new platforms for realizing chiral TSC, observing Majorana zero modes, and executing TQC.

Note added.—After the submission of this Letter, a related paper focusing on the RKKY interaction appeared [30]. A closer comparison between the two studies is made in the Supplemental Material [24].

*zhangzy@ustc.edu.cn

[1] A. Y. Kitaev, Ann. Phys. (Amsterdam) **303**, 2 (2003).
[2] C. Nayak, S. H. Simon, A. Stern, M. Freedman, and S. Das Sarma, Rev. Mod. Phys. **80**, 1083 (2008).
[3] G. Moore and N. Read, Nucl. Phys. **B360**, 362 (1991).
[4] X. L. Qi and S. C. Zhang, Rev. Mod. Phys. **83**, 1057 (2011).
[5] L. J. Buchholtz and G. Zwicknagl, Phys. Rev. B **23**, 5788 (1981).
[6] M. Matsumoto and M. Sigrist, J. Phys. Soc. Jpn. **68**, 994 (1999).
[7] X. L. Qi, T. L. Hughes, and S. C. Zhang, Phys. Rev. B **82**, 184516 (2010).
[8] D. A. Ivanov, Phys. Rev. Lett. **86**, 268 (2001).
[9] N. Read and D. Green, Phys. Rev. B **61**, 10267 (2000).
[10] L. Fu and C. L. Kane, Phys. Rev. Lett. **100**, 096407 (2008); Phys. Rev. B **79**, 161408 (2009).
[11] J. D. Sau, R. M. Lutchyn, S. Tewari, and S. Das Sarma, Phys. Rev. Lett. **104**, 040502 (2010).
[12] J. Alicea, Phys. Rev. B **81**, 125318 (2010).
[13] V. Mourik, K. Zuo, S. M. Frolov, S. R. Plissard, E. P. A. M. Bakkers, and L. P. Kouwenhoven, Science **336**, 1003 (2012).
[14] A. Das, Y. Ronen, Y. Most, Y. Oreg, M. Heiblum, and H. Shtrikman, Nat. Phys. **8**, 887 (2012).
[15] M. T. Deng, C. L. Yu, G. Y. Huang, M. Larsson, P. Caroff, and H. Q. Xu, Nano Lett. **12**, 6414 (2012).
[16] D. Xiao, M. C. Chang, and Q. Niu, Rev. Mod. Phys. **82**, 1959 (2010).
[17] H. Zhang, C.-X. Liu, X.-L. Qi, X. Dai, Z. Fang, and S.-C. Zhang, Nat. Phys. **5**, 438 (2009).
[18] Q. Liu, C. X. Liu, C. K. Xu, X. L. Qi, and S. C. Zhang, Phys. Rev. Lett. **102**, 156603 (2009).
[19] J. S. Dyck, P. Hájek, P. Lošt'ák, and C. Uher, Phys. Rev. B **65**, 115212 (2002).
[20] J. J. Zhu, D. X. Yao, S. C. Zhang, and K. Chang, Phys. Rev. Lett. **106**, 097201 (2011).
[21] L. Yu, Acta Phys. Sin. **21**, 75 (1965).
[22] H. Shiba, Prog. Theor. Phys. **40**, 435 (1968).
[23] A. V. Balatsky, I. Vekhter, and J. X. Zhu, Rev. Mod. Phys. **78**, 373 (2006).
[24] See Supplemental Material at http://link.aps.org/supplemental/10.1103/PhysRevLett.113.266806, which includes Refs. [22,23,25,30], for details of the analytical derivations and a more thorough discussion on the in-plane magnetization.
[25] A. A. Abrikosov and L. P. Gor'kov, Zh. Eksp. Teor. Fiz. **39**, 1781 (1960) [Sov. Phys. JETP **12**, 1243 (1961)].
[26] G. Bouzerar, J. Kudrnovský, L. Bergqvist, and P. Bruno, Phys. Rev. B **68**, 081203(R) (2003).
[27] H. Chen, W. G. Zhu, E. Kaxiras, and Z. Y. Zhang, Phys. Rev. B **79**, 235202 (2009).
[28] M. X. Wang et al., Science **336**, 52 (2012).
[29] E. Wang et al., Nat. Phys. **9**, 621 (2013).
[30] A. A. Zyuzin and D. Loss, Phys. Rev. B **90**, 125443 (2014).